Journal of Zhejiang University SCIENCE A
ISSN 1673-565X (Print); ISSN 1862-1775 (Online)
www.zju.edu.cn/jzus; www.springerlink.com
E-mail: jzus@zju.edu.cn

Proportional integral plus multi-frequency resonant current controller for grid-connected voltage source converter under imbalanced and distorted supply voltage conditions*

Jia-bing HU[1], Wei ZHANG‡[1], Hong-sheng WANG[1], Yi-kang HE[1], Lie XU[2]

([1]*School of Electrical Engineering, Zhejiang University, Hangzhou 310027, China*)

([2]*Department of Electronics and Electrical Engineering, Strathclyde University, Glasgow G1 1XW, UK*)

E-mail: {emec_zju, weizhang, homeson_wang, ykhe}@zju.edu.cn; lie.xu@eee.strath.ac.uk

Received June 12, 2008; Revision accepted Dec. 25, 2008; Crosschecked July 30, 2009

Abstract: This paper proposes a current control scheme for a grid-connected pulse width modulator (PWM) voltage source converter (GC-VSC) under imbalanced and distorted supply voltage conditions. The control scheme is implemented in the positive synchronously rotating reference frame and composed of a single proportional integral (PI) regulator and multi-frequency resonant controllers tuned at the frequencies of 2ω and 6ω, respectively. The experimental results, with the target of eliminating the active power oscillations and current harmonics on a prototype GC-VSC system, validate the feasibility of the proposed current control scheme during supply voltage imbalance and distortion.

Key words: Grid-connected voltage source converter (GC-VSC), Proportional integral plus multi-frequency resonant (PI+MFR), Imbalance, Harmonics distortion

doi:10.1631/jzus.A0820440 **Document code:** A **CLC number:** TM315; TM614

INTRODUCTION

The three-phase pulse width modulator (PWM) voltage source converter (VSC) connected to the grid can be used in several applications, namely as bidirectional ac/dc rectifiers in the power supply for electrical motor drives, for distributed power generation with renewable energy sources including wind, hydro and solar energy, as active power filters and micro-grid power conditioners. Recently, current control of the grid-connected VSC (GC-VSC) has been one of the most important research subjects. A general review of the available current control techniques for the GC-VSC was reported in Kazmierkowski *et al*.(2002), which classified them into two groups, viz., linear and nonlinear controllers. Among them, proportional integral (PI) current control with supply voltage feedforward in the synchronous *dq* reference frame rotating at the grid angular frequency (single PI) is one alternative (Verdelho and Marques, 1998). In addition, the proportional resonant (PR) controller is developed for precise current reference tracking in the stationary frame, which also achieves similar frequency response characteristics to the synchronous PI control (Zmood and Holmes, 2003). The basic functionality of the PR controller is to introduce an infinite gain at a tuned resonant frequency for eliminating the steady-state error at that frequency, which is conceptually similar to an integrator whose infinite dc gain forces the dc steady-state error to null. Therefore, it was proven in Yuan *et al*.(2002) that the resonant term of the PR controller can be recognized as a generalized ac integrator.

However, once the supply voltage disturbances (i.e., imbalance and harmonics distortion) occur, the

‡ Corresponding author

* Project supported by the National Natural Science Foundation of China (No. 50907057) and the National High-Tech Research and Development Program (863) of China (No. 2007AA05Z419)

control scheme using a single PI or PR controller leads to deficient current control and deteriorated performance of the converters, including low-frequency harmonics in the ac current and significant oscillations in the dc link voltage and active/reactive powers. As a result, various control structures have been proposed in the last decade, which are aimed at improving the GC-VSC's operation under imbalanced supply voltage conditions (Rioual *et al*., 1996; Song and Nam, 1999; Suh and Lipo, 2006; Hu *et al.*, 2007; Hu and He, 2007; 2008; Wu *et al*., 2008; Yin *et al*., 2008). In Rioual *et al*.(1996), a control strategy for eliminating dc link voltage ripples is proposed using the single PI current controller in the positive synchronously rotating reference frame and an added real-time voltage feedforward implemented in the negative synchronously rotating reference frame. Thus, the additional capability for voltage disturbance rejection enables the elimination of active power oscillations at the grid connection point, whereas the main drawback of this control scheme is its limited bandwidth. Furthermore, a dual current control scheme was presented in (Song and Nam, 1999; Hu *et al.*, 2007; Wu *et al*., 2008; Yin *et al*., 2008), which contains a PI controller in the positive synchronous frame for regulating the positive-sequence current and another controller in the negative synchronous frame for the negative-sequence current. In this case, real-time sequential decomposition methods for both voltage and current are essential to obtain appropriate current references and to control them in their respective (positive and negative) reference frames. Nevertheless, the employed decomposing method in (Song and Nam, 1999; Hu *et al.*, 2007; Wu *et al*., 2008; Yin *et al*., 2008) using a notch filter considerably limits the transient behavior of the system, which makes it suitable only for steady-state applications. To solve this problem, a multi-frequency PR controller implemented in the stationary frame was proposed in Hu and He (2007; 2008) for regulating GC-VSC's negative sequence current during supply voltage imbalance. Alternatively, a modified dual control scheme was presented in Suh and Lipo (2006), in which a resonant regulator tuned at double the grid frequency was added at each of the reference frames to deal with the opposite sequence. However, as far as the authors know, there have been few reports of current control schemes of GC-VSC under both imbalanced and harmonically distorted supply voltage conditions, which are common in modern distribution networks.

It is worth noting that the generalized ac integrator (R) is a double integrator, which means that a resonant part tuned at the angular frequency of ω is able to nullify the error not only for the component at the frequency of ω but also for the harmonic at $-\omega$. Typically, the harmonics considered in the supply voltage are ω (fundamental), $-\omega$ (imbalance), -5ω, 7ω, etc. Therefore, this paper presents an improved current control scheme using a PI plus multi-frequency resonant (PI+MFR) controller for GC-VSC under imbalanced and distorted supply voltage conditions.

BEHAVIOUR OF THE GC-VSC SYSTEM

The schematic diagram of a typical three-phase grid-connected PWM VSC is shown in Fig.1.

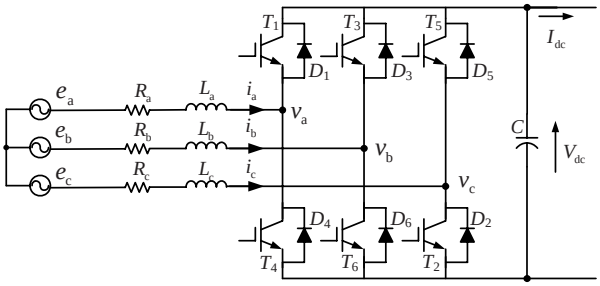

Fig.1 Schematic diagram of a three-phase grid-connected voltage source converter

The behavior for the ac side of the GC-VSC can be described in terms of voltage and current in the positive synchronous dq^+ reference frame rotating at an angular speed of ω as

$$\boldsymbol{E}_{dq}^{+}=L\frac{\mathrm{d}\boldsymbol{I}_{dq}^{+}}{\mathrm{d}t}+R\boldsymbol{I}_{dq}^{+}+\mathrm{j}\omega L\boldsymbol{I}_{dq}^{+}+\boldsymbol{V}_{dq}^{+}, \tag{1}$$

where superscript '+' represents the positive synchronous reference frame. $\boldsymbol{E}_{dq}^{+}=E_d^{+}+\mathrm{j}E_q^{+}$, $\boldsymbol{V}_{dq}^{+}=V_d^{+}+\mathrm{j}V_q^{+}$ and $\boldsymbol{I}_{dq}^{+}=I_d^{+}+\mathrm{j}I_q^{+}$ are the respective space vectors of the ac input supply voltages, the VSC input pole voltages and the ac input currents in the positive dq^+ frame. L_a=L_b=L_c=L and R_a=R_b=R_c=R are the three-phase VSC input inductors and resistors, respectively.

Under imbalanced and distorted supply conditions, no zero-sequence component is assumed, and the positive/negative sequence of the fundamental frequency and the harmonics at the frequencies of -5ω and 7ω are taken into account in this paper. Hence the voltage and current vectors can be expressed in terms of the positive/negative sequence and the harmonic components in the dq^+ frame as

$$\boldsymbol{F}_{dq}^{+}=\boldsymbol{F}_{dq+}^{+}+\boldsymbol{F}_{dq-}^{-}\mathrm{e}^{-\mathrm{j}2\omega t}+\boldsymbol{F}_{dq5-}^{5-}\mathrm{e}^{-\mathrm{j}6\omega t}+\boldsymbol{F}_{dq7+}^{7+}\mathrm{e}^{\mathrm{j}6\omega t}, \quad (2)$$

where $\boldsymbol{F}$ represents, in a broad sense, the voltage and current; subscripts '+', '−' represent the positive and negative rotating reference frames at ω and $-\omega$, respectively; $\boldsymbol{F}_{dq5-}^{5-}$ refers to the 5th harmonic quantity in the synchronous reference frame rotating at the angular speed of -5ω. It is worth noting that -5ω and 7ω harmonics both behave as the ac components at the speed of $\pm6\omega$ in the dq^+ reference frame.

The output active and reactive powers at the grid connection point can be expressed as

$$\begin{aligned}P+\mathrm{j}Q&=-\frac{3}{2}\boldsymbol{E}_{dq}^{+}\hat{\boldsymbol{I}}_{dq}^{+}\\&=-\frac{3}{2}\left(\boldsymbol{E}_{dq+}^{+}+\boldsymbol{E}_{dq-}^{-}\mathrm{e}^{-\mathrm{j}2\omega t}+\boldsymbol{E}_{dq5-}^{5-}\mathrm{e}^{-\mathrm{j}6\omega t}+\boldsymbol{E}_{dq7+}^{7+}\mathrm{e}^{\mathrm{j}6\omega t}\right)\\&\quad\cdot\left(\hat{\boldsymbol{I}}_{dq+}^{+}+\hat{\boldsymbol{I}}_{dq-}^{-}\mathrm{e}^{\mathrm{j}2\omega t}+\hat{\boldsymbol{I}}_{dq5-}^{5-}\mathrm{e}^{\mathrm{j}6\omega t}+\hat{\boldsymbol{I}}_{dq7+}^{7+}\mathrm{e}^{-\mathrm{j}6\omega t}\right).\end{aligned} \quad (3)$$

It is shown that during supply voltage imbalance and harmonic distortions, the active and reactive powers of GC-VSC both contain additional oscillations at the frequencies of 2ω, 4ω, 6ω, 8ω and 12ω. Thus, Eq.(3) can be rearranged as

$$\begin{aligned}P&=P_0+P_{\cos2}\cos(2\omega t)+P_{\sin2}\sin(2\omega t)+P_{\cos4}\cos(4\omega t)\\&\quad+P_{\sin4}\sin(4\omega t)+P_{\cos6}\cos(6\omega t)+P_{\sin6}\sin(6\omega t)\\&\quad+P_{\cos8}\cos(8\omega t)+P_{\sin8}\sin(8\omega t)+P_{\cos12}\cos(12\omega t)\\&\quad+P_{\sin12}\sin(12\omega t),\end{aligned} \quad (4a)$$

$$\begin{aligned}Q&=Q_0+Q_{\cos2}\cos(2\omega t)+Q_{\sin2}\sin(2\omega t)+Q_{\cos4}\cos(4\omega t)\\&\quad+Q_{\sin4}\sin(4\omega t)+Q_{\cos6}\cos(6\omega t)+Q_{\sin6}\sin(6\omega t)\\&\quad+Q_{\cos8}\cos(8\omega t)+Q_{\sin8}\sin(8\omega t)+Q_{\cos12}\cos(12\omega t)\\&\quad+Q_{\sin12}\sin(12\omega t),\end{aligned} \quad (4b)$$

where average and oscillating items P_0, $P_{\cos2}$, $P_{\sin2}$, $P_{\cos4}$, $P_{\sin4}$, $P_{\cos6}$, $P_{\sin6}$, $P_{\cos8}$, $P_{\sin8}$, $P_{\cos12}$, $P_{\sin12}$ and Q_0, $Q_{\cos2}$, $Q_{\sin2}$, $Q_{\cos4}$, $Q_{\sin4}$, $Q_{\cos6}$, $Q_{\sin6}$, $Q_{\cos8}$, $Q_{\sin8}$, $Q_{\cos12}$, $Q_{\sin12}$ are given by Eqs.(4c)~(4g).

$$\begin{bmatrix}P_{\cos2}\\P_{\sin2}\\Q_{\cos2}\\Q_{\sin2}\end{bmatrix}=-\frac{3}{2}\begin{bmatrix}E_{d-}^{-}&E_{q-}^{-}&E_{d+}^{+}&E_{q+}^{+}\\E_{q-}^{-}&-E_{d-}^{-}&-E_{q+}^{+}&E_{d+}^{+}\\E_{q-}^{-}&-E_{d-}^{-}&E_{q+}^{+}&-E_{d+}^{+}\\-E_{d-}^{-}&-E_{q-}^{-}&E_{d+}^{+}&E_{q+}^{+}\end{bmatrix}\begin{bmatrix}I_{d+}^{+}\\I_{q+}^{+}\\I_{d-}^{-}\\I_{q-}^{-}\end{bmatrix}, \quad (4d)$$

$$\begin{bmatrix}P_{\cos4}\\P_{\sin4}\\Q_{\cos4}\\Q_{\sin4}\end{bmatrix}=-\frac{3}{2}\begin{bmatrix}E_{d5-}^{5-}&E_{q5-}^{5-}&E_{d-}^{-}&E_{q-}^{-}\\E_{q5-}^{5-}&-E_{d5-}^{5-}&-E_{q-}^{-}&E_{d-}^{-}\\E_{q5-}^{5-}&-E_{d5-}^{5-}&E_{q-}^{-}&-E_{d-}^{-}\\-E_{d5-}^{5-}&-E_{q5-}^{5-}&E_{d-}^{-}&E_{q-}^{-}\end{bmatrix}\begin{bmatrix}I_{d+}^{+}\\I_{q+}^{+}\\I_{d5-}^{5-}\\I_{q5-}^{5-}\end{bmatrix}, \quad (4e)$$

$$\begin{bmatrix}P_{\cos8}\\P_{\sin8}\\Q_{\cos8}\\Q_{\sin8}\end{bmatrix}=-\frac{3}{2}\begin{bmatrix}E_{d7+}^{7+}&E_{q7+}^{7+}&E_{d-}^{-}&E_{q-}^{-}\\-E_{q7+}^{7+}&E_{d7+}^{7+}&E_{q-}^{-}&-E_{d-}^{-}\\E_{q7+}^{7+}&-E_{d7+}^{7+}&E_{q-}^{-}&-E_{d-}^{-}\\E_{d7+}^{7+}&E_{q7+}^{7+}&-E_{d-}^{-}&-E_{q-}^{-}\end{bmatrix}\begin{bmatrix}I_{d-}^{-}\\I_{q-}^{-}\\I_{d7+}^{7+}\\I_{q7+}^{7+}\end{bmatrix}, \quad (4f)$$

$$\begin{bmatrix}P_{\cos12}\\P_{\sin12}\\Q_{\cos12}\\Q_{\sin12}\end{bmatrix}=-\frac{3}{2}\begin{bmatrix}E_{d7+}^{7+}&E_{q7+}^{7+}&E_{d5-}^{5-}&E_{q5-}^{5-}\\-E_{q7+}^{7+}&E_{d7+}^{7+}&E_{q5-}^{5-}&-E_{d5-}^{5-}\\E_{q7+}^{7+}&-E_{d7+}^{7+}&E_{q5-}^{5-}&-E_{d5-}^{5-}\\E_{d7+}^{7+}&E_{q7+}^{7+}&-E_{d5-}^{5-}&-E_{q5-}^{5-}\end{bmatrix}\begin{bmatrix}I_{d5-}^{5-}\\I_{q5-}^{5-}\\I_{d7+}^{7+}\\I_{q7+}^{7+}\end{bmatrix}. \quad (4g)$$

$$\begin{bmatrix}P_0\\Q_0\\P_{\cos6}\\P_{\sin6}\\Q_{\cos6}\\Q_{\sin6}\end{bmatrix}=-\frac{3}{2}\begin{bmatrix}E_{d+}^{+}&E_{q+}^{+}&E_{d-}^{-}&E_{q-}^{-}&E_{d5-}^{5-}&E_{q5-}^{5-}&E_{d7+}^{7+}&E_{q7+}^{7+}\\E_{q+}^{+}&-E_{d+}^{+}&E_{q-}^{-}&-E_{d-}^{-}&E_{q5-}^{5-}&-E_{d5-}^{5-}&E_{q7+}^{7+}&-E_{d7+}^{7+}\\E_{d5-}^{5-}+E_{d7+}^{7+}&E_{q5-}^{5-}+E_{q7+}^{7+}&0&0&E_{d+}^{+}&-E_{q+}^{+}&E_{d+}^{+}&E_{q+}^{+}\\-E_{q5-}^{5-}+E_{q7+}^{7+}&E_{d5-}^{5-}-E_{d7+}^{7+}&0&0&E_{d+}^{+}&E_{q+}^{+}&E_{d+}^{+}&E_{q+}^{+}\\E_{q5-}^{5-}-E_{q7+}^{7+}&-E_{d5-}^{5-}-E_{d7+}^{7+}&0&0&E_{q+}^{+}&-E_{d+}^{+}&E_{q+}^{+}&-E_{d+}^{+}\\-E_{q5-}^{5-}+E_{q7+}^{7+}&E_{d5-}^{5-}-E_{d7+}^{7+}&0&0&E_{q+}^{+}&-E_{d+}^{+}&-E_{q+}^{+}&E_{d+}^{+}\end{bmatrix}\begin{bmatrix}I_{d+}^{+}\\I_{q+}^{+}\\I_{d-}^{-}\\I_{q-}^{-}\\I_{d5-}^{5-}\\I_{q5-}^{5-}\\I_{d7+}^{7+}\\I_{q7+}^{7+}\end{bmatrix} \quad (4c)$$

Consequently, using the power-balancing equation, the equation for the dc link under the imbalanced and distorted conditions can be expressed as

$$P = C_{\mathrm{dc}} \frac{\mathrm{d}V_{\mathrm{dc}}}{\mathrm{d}t} + I_{\mathrm{dc}} V_{\mathrm{dc}}. \tag{5}$$

Therefore, Eqs.(4) and (5) can be used to represent the ac and dc side system model for the three-phase GC-VSC under imbalanced and distorted supply conditions.

CONTROL STRATEGY FOR GC-VSC DURING VOLTAGE IMBALANCE AND DISTORTION

As shown in Eq.(2), under imbalanced and distorted supply conditions, the GC-VSC's current contains positive and negative sequence components as well as the 5th and 7th order harmonics. In this paper, one of the control targets is set to eliminate the current harmonics, viz., $\boldsymbol{I}_{dq5-}^{5-*} = \boldsymbol{0}$ and $\boldsymbol{I}_{dq7+}^{7+*} = \boldsymbol{0}$. As expressed in Eq.(4), once the current harmonics are nullified, the oscillations at 4ω, 6ω and 8ω in the active and reactive powers can be decreased, and the 12ω components are totally removed.

As expressed in Eq.(4), besides $\boldsymbol{I}_{dq5-}^{5-}$ and $\boldsymbol{I}_{dq7+}^{7+}$, another four variables, i.e., I_{d+}^{+}, I_{q+}^{+}, I_{d-}^{-} and I_{q-}^{-}, can be regulated. Apart from controlling the average active and reactive powers, i.e., P_0 and Q_0, two more variables can be controlled. As a bidirectional ac/dc rectifier, the GC-VSC system should be designed to eliminate the 2ω pulsations in the dc-link voltage, which is equivalent to nullifying the active power oscillations and is recognized as the second control target in this study. Thus, the oscillating terms in the active power shown in Eq.(4d) have to be zero, i.e., $P_{\cos 2}$=0 and $P_{\sin 2}$=0.

As the d^+-axis is fixed to be with the positive input voltage vector in the supply voltage orientation, i.e., $E_{q+}^{+} = 0$, the reference values of the negative-sequence currents for the proposed control strategy can be calculated by

$$\begin{bmatrix} I_{d+}^{+*} \\ I_{q+}^{+*} \\ I_{d-}^{-*} \\ I_{q-}^{-*} \end{bmatrix} = -\frac{2}{3} \begin{bmatrix} E_{d+}^{+} & 0 & E_{d-}^{-} & E_{q-}^{-} \\ 0 & -E_{d+}^{+} & -E_{q-}^{-} & E_{d-}^{-} \\ E_{d-}^{-} & E_{q-}^{-} & E_{d+}^{+} & 0 \\ E_{q-}^{-} & -E_{d-}^{-} & 0 & E_{d+}^{+} \end{bmatrix}^{-1} \begin{bmatrix} P_0^* \\ Q_0^* \\ 0 \\ 0 \end{bmatrix}. \tag{6}$$

For clear illustration, the results are simplified and synthesized in Table 1.

Table 1 Positive/Negative sequence and harmonic current references

Current	Value	Current	Value
I_{d+}^{+*}	$2E_{d+}^{+}P_0/(3K_1)$	I_{d5-}^{5-*}	0
I_{q+}^{+*}	$2E_{d+}^{+}Q_0/(3K_2)$	I_{q5-}^{5-*}	0
I_{d-}^{-*}	$-k_{dd}I_{d+}^{+*} - k_{qd}I_{q+}^{+*}$	I_{d7+}^{7+*}	0
I_{q-}^{-*}	$-k_{qd}I_{d+}^{+*} + k_{dd}I_{q+}^{+*}$	I_{q7+}^{7+*}	0

Note: $K_1 = (E_{d+}^{+})^2 - (E_{d-}^{-})^2 - (E_{q-}^{-})^2$, $K_2 = (E_{d+}^{+})^2 + (E_{d-}^{-})^2 + (E_{q-}^{-})^2$, $k_{dd} = E_{d-}^{-}/E_{d+}^{+}$, and $k_{qd} = E_{q-}^{-}/E_{d+}^{+}$

CURRENT CONTROL SCHEME

Proportional integral plus multi-frequency resonant (PI+MFR) controllers

Once the references of the positive- and negative-sequence and harmonic currents are determined, it is vitally important that the current controllers control both the positive- and negative-sequence and harmonic components rapidly and accurately. This paper presents a new current control scheme, which consists of a single PI and multi-frequency resonant (PI+MFR) controllers in the positive synchronous dq^+ reference frame, as shown in Fig.2. The resonant controllers are tuned at 2ω and 6ω, respectively, for the purpose of introducing an infinite gain at the selected resonant frequencies. As a result, the proposed PI+MFR controller forces the steady-state errors to be null for both positive/negative sequence currents and 5th/7th order harmonics.

According to Eq.(1), the control system for the GC-VSC's currents in the supply voltage oriented synchronous dq^+ reference frame can be designed. Without any decomposition processes for positive/negative sequence or harmonic currents, the required control voltage $\boldsymbol{V}_{dq}^{+}$ can be calculated as

$$\boldsymbol{V}_{dq}^{+}=-L\boldsymbol{U}_{dq}^{+}+\boldsymbol{E}_{dq}^{+}-R\boldsymbol{I}_{dq}^{+}-\mathrm{j}\omega L\boldsymbol{I}_{dq}^{+}, \tag{7}$$

where

$$\begin{aligned}\boldsymbol{U}_{dq}^{+}&=\frac{\mathrm{d}}{\mathrm{d}t}\boldsymbol{I}_{dq}^{+}=C_{\text{PI-RES}}(s)(\boldsymbol{I}_{dq}^{+*}-\boldsymbol{I}_{dq}^{+})\\&=\left(K_{i\mathrm{P}}+\frac{K_{i\mathrm{I}}}{s}+\frac{sK_{i\mathrm{R1}}}{s^2+2\omega_{\mathrm{c}1}s+(2\omega)^2}\right.\\&\quad\left.+\frac{sK_{i\mathrm{R2}}}{s^2+2\omega_{\mathrm{c}2}s+(6\omega)^2}\right)(\boldsymbol{I}_{dq}^{+*}-\boldsymbol{I}_{dq}^{+}),\end{aligned}$$

$K_{i\mathrm{P}}$, $K_{i\mathrm{I}}$, $K_{i\mathrm{R1}}$ and $K_{i\mathrm{R2}}$ are the proportional, integral, and resonant gains, respectively, and $\omega_{\mathrm{c}1}$ and $\omega_{\mathrm{c}2}$ are the cut-off frequencies.

Fig.2 shows the control scheme of PI+MFR controllers with R parts tuned at 2ω and 6ω, respectively. Fig.3 presents the zeros and eigenvalues of the system transfer function $\boldsymbol{I}_{dq}^{+}/\boldsymbol{I}_{dq}^{+*}$ with conventional single PI and the proposed PI+MFR controllers, respectively. For a switching frequency of 2.5 kHz, the system response is designed at ω_{n}=2370 rad/s with

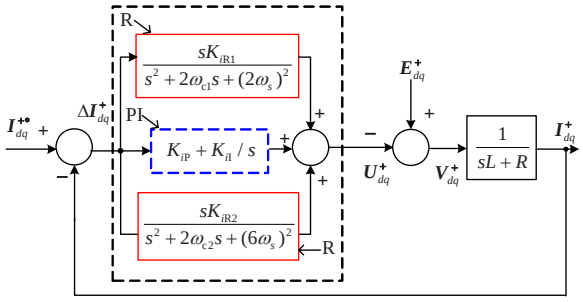

Fig.2 Proportional integral (PI) plus multi-frequency resonant controller in the dq^{+} reference frame

$\omega_{\mathrm{c}1}$=$\omega_{\mathrm{c}2}$=2.0 rad/s, $K_{i\mathrm{R1}}$=$K_{i\mathrm{R2}}$=500 and system damping ξ=0.707. As can be seen from Fig.3b, the system transfer function by using PI+MFR is composed of a dominant real zero at −1725.9, two dominant complex eigenvalues at −1680±j1710 as well as four non-dominant complex zeros at −18.5±j1888 and −4.5±j622.2 and eigenvalues at −12.1±j187.6 and −4.2±j622.2, respectively. Thus, the system stability with the PI+MFR controller used can be determined by its dominant zero and eigenvalues, which is similar to the one using a single PI controller, as shown in Fig.3a.

The GC-VSC's control voltage is then transformed from the synchronous dq^{+} frame to the stationary frame as

$$\boldsymbol{V}_{\alpha\beta}=\boldsymbol{V}_{dq}^{+}\mathrm{e}^{\mathrm{j}\theta}. \tag{8}$$

System implementation

Fig.4 shows the proposed current control scheme for GC-VSC under imbalanced and distorted supply voltage conditions. As shown, without involving any sequential-component decomposition, the measured and transformed currents fed to the current controller consist of the dc value and ac components at the frequencies of 2ω and 6ω. However, the current references given in Table 1 are all dc signals separated in their respective reference frames. Therefore, it is necessary to transform the reference values to the positive synchronous dq^{+} reference frame. According to Eq.(2), the current references are calculated as

$$\boldsymbol{I}_{dq}^{+*}=\boldsymbol{I}_{dq+}^{+*}+\boldsymbol{I}_{dq-}^{-*}\mathrm{e}^{-\mathrm{j}2\theta}+\boldsymbol{I}_{dq5-}^{5-*}\mathrm{e}^{-\mathrm{j}6\theta}+\boldsymbol{I}_{dq7+}^{7+*}\mathrm{e}^{\mathrm{j}6\theta}. \tag{9}$$

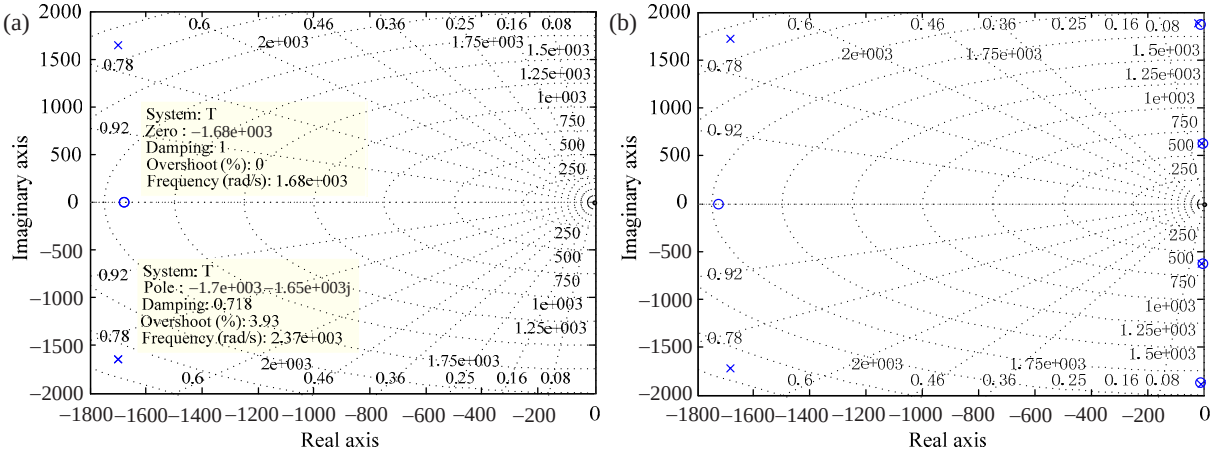

Fig.3 Eigenvalues and zeros of the current control system

(a) Single PI controller; (b) PI plus multi-frequency resonant controllers

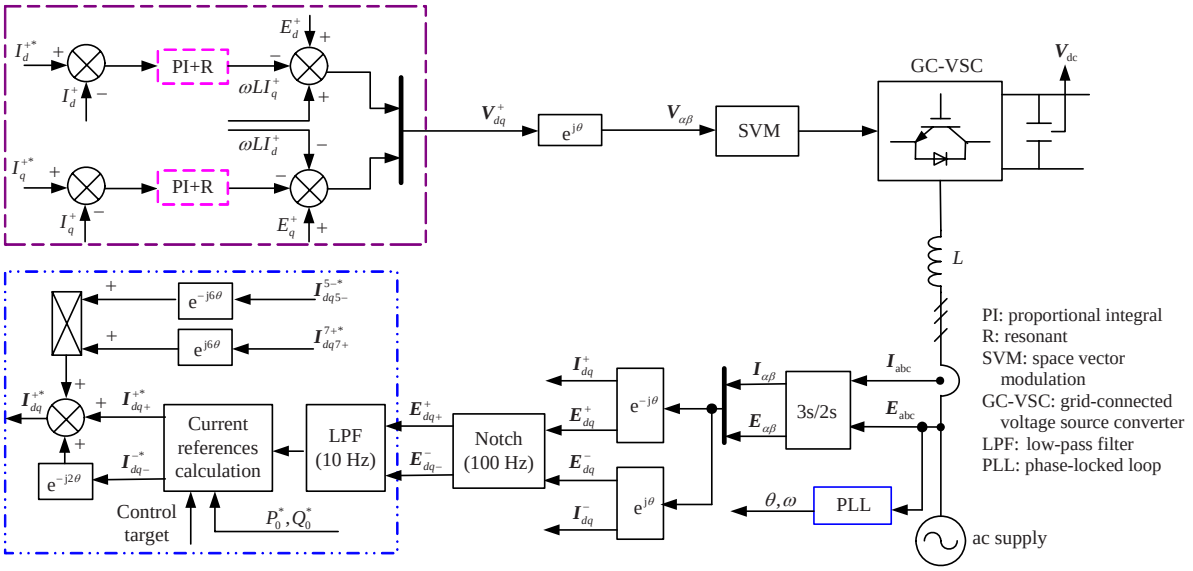

Fig.4 The proposed current control scheme of GC-VSC during supply imbalance and distortion

EXPERIMENTAL RESULTS

Experimental tests were performed in a 2.0 kW GC-VSC test rig and Fig.5 shows the schematic diagram of the experimental system. As shown, the voltage imbalance during the tests was generated using three single-phase variacs. The voltage imbalance was around 18% and the pre-existing 5th and 7th harmonics in the supply voltage were 0.9% and 0.35%, respectively. The GC-VSC was controlled by a TI TMS320F2812 DSP. The switching frequency of the converter was set at 2.5 kHz. Asymmetric space vector modulation (SVM) was used for switching pulse generation with a sampling frequency of 10 kHz. The line inductance and resistance are 4.0 mH and 0.2 Ω, respectively. In order to examine the transient response of the proposed current control strategy, the common dc link voltage was fixed at 200 V. Under such conditions, the GC-VSC operated as a grid-connected inverter.

Fig.6 shows the experimental results using the conventional single PI, the proposed PI+R controller tuned at 100 Hz and PI+MFR controllers tuned at 100 and 300 Hz, respectively. As shown in Fig.6a, the conventional single PI resulted in significant active and reactive power oscillations with little control on negative sequence currents during the supply voltage imbalance. Even worse, the currents contained

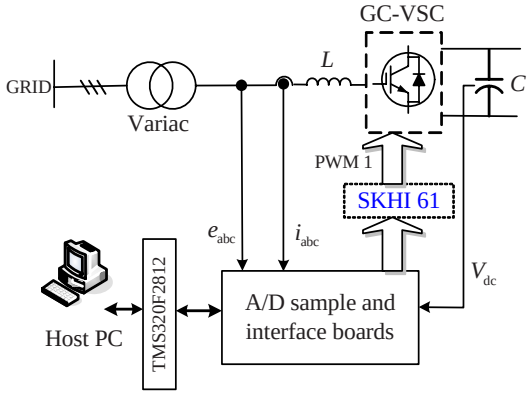

Fig.5 Schematic diagram of the experimental system

significant 5th and 7th order harmonics (1.38% and 1.59%, respectively). As shown in Fig.6b, once the proposed PI+R controller tuned at 100 Hz was employed with the positive and negative sequence current references listed in Table 1, the oscillations in the active power were eliminated whereas the current harmonics still existed. While the proposed PI+MFR controller tuned at 100 and 300 Hz was used with all the current references listed in Table 1, both active power oscillations as well as the 5th and 7th order current harmonics were totally eliminated, as shown in Fig.6c. It is noted from Figs.6b and 6c that the oscillations in reactive power still existed due to the limited control variables, as expressed in Eq.(4) (Hu and He, 2008).

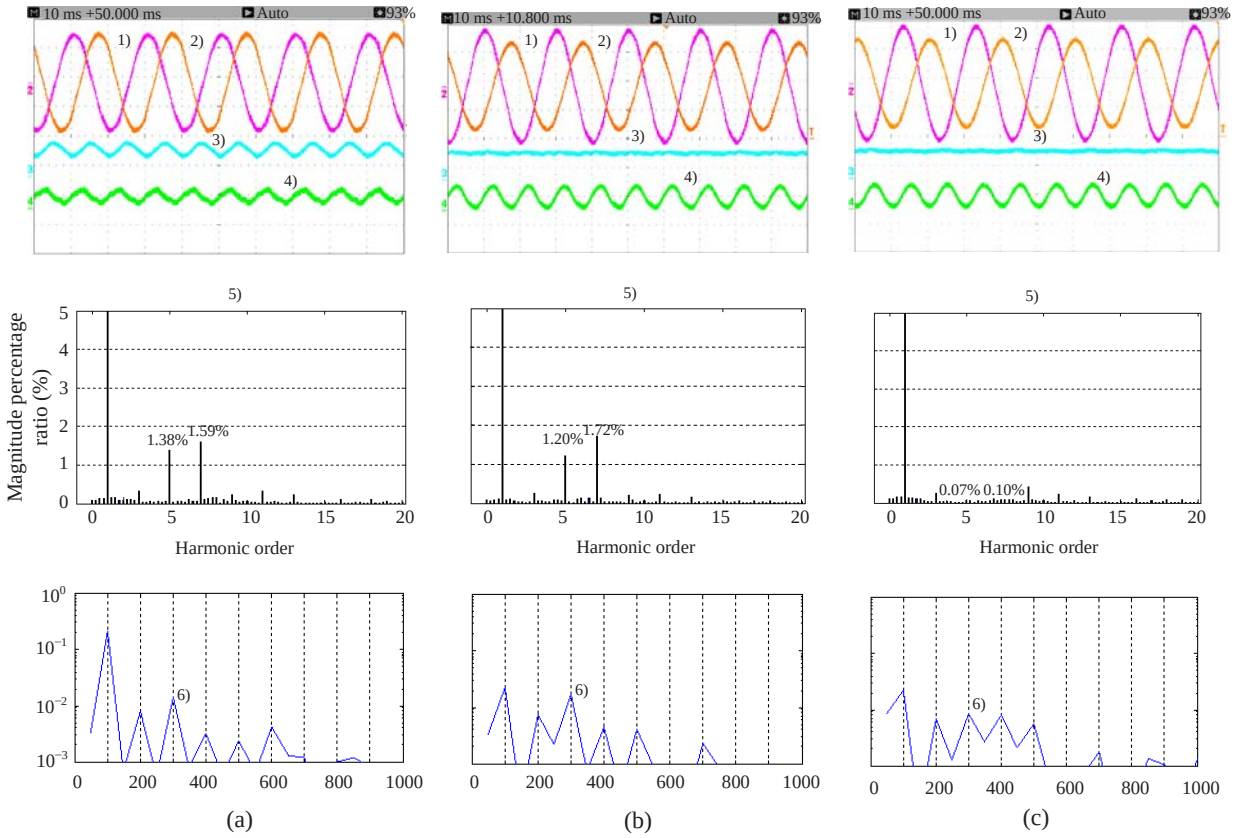

Fig.6 Experimental results with I_{d+}^{+*}=7.5 A (peak) (*P* generating) and I_{q+}^{+*}=3.0 A (peak) (*Q* generating) during 18.0% supply voltage imbalance and 5th and 7th voltage harmonics being 0.9% and 0.35%, respectively

(a) Single PI; (b) PI plus resonant controller tuned at 100 Hz; (c) PI plus multi-frequency resonant controllers tuned at 100 and 300 Hz. 1) i_a (5 A/div); 2) i_b (5 A/div); 3) *P* (2 kW/div); 4) *Q* (2 kvar/div); 5) i_a spectrum, percentage ratio of the harmonics magnitude to the fundamental magnitude (%); 6) *P* spectrum

Further tests with various active and reactive power step changes were conducted using different current control schemes under imbalanced and distorted supply voltage conditions and Figs.7 and 8 show the measured results. As shown in Figs.7a and 8a, the conventional single PI current control scheme was not capable of controlling the negative sequence currents efficiently under either steady state or transient conditions, which led to significant power oscillations. It is worth noting that for the results presented in Figs.7a and 8a, the negative sequence current references were not zero but the values presented in Table 1. Consequently, the active power oscillations got reduced compared with that shown in Fig.6a. It is obvious by comparison that the proposed PI+R and PI+MFR current control schemes not only provided pretty good system performance with null steady-state errors for the negative sequence as well as 5th and 7th order harmonic currents, but also maintained identically transient responses to that of a single PI controller. It can be measured from the results in Figs.7 and 8 that the dynamic responses of both active and reactive powers were within around 5 ms. As a result, the system performance using the proposed current control schemes was satisfactory with active power oscillations and 5th/7th order current harmonics eliminated during supply voltage imbalance and harmonic distortions.

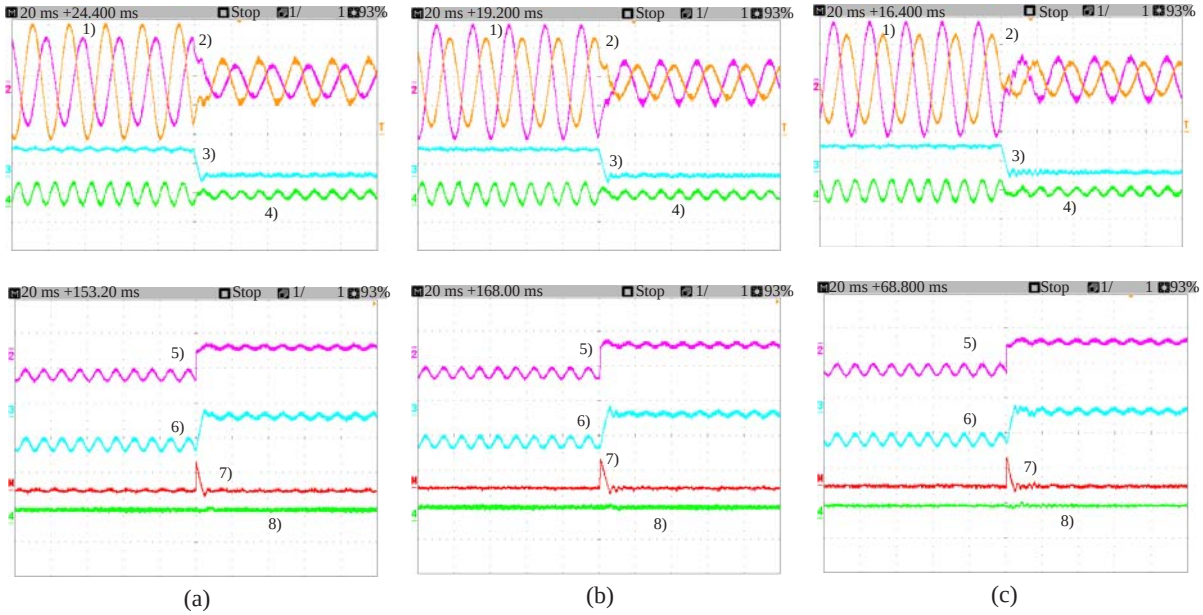

Fig.7 Experimental results with I_{q+}^{+*} =3.0 A (peak) and I_{d+}^{+*} step changed from −7.5 A (peak) to 0 during 18.0% supply voltage imbalance and 5th and 7th order voltage harmonics being 0.9% and 0.35%, respectively

(a) Single PI; (b) PI plus resonant controller tuned at 100 Hz; (c) PI plus multi-frequency resonant controllers tuned at 100 and 300 Hz. 1) i_a (5 A/div); 2) i_b (5 A/div); 3) P (2 kW/div); 4) Q (2 kvar/div); 5) I_{gd}^{+*} (9 A/div); 6) I_{gd}^{+} (9 A/div); 7) $\Delta I_{gd}^{+} = I_{gd}^{+*} - I_{gd}^{+}$ (9 A/div); 8) I_{gq+}^{+} (9 A/div)

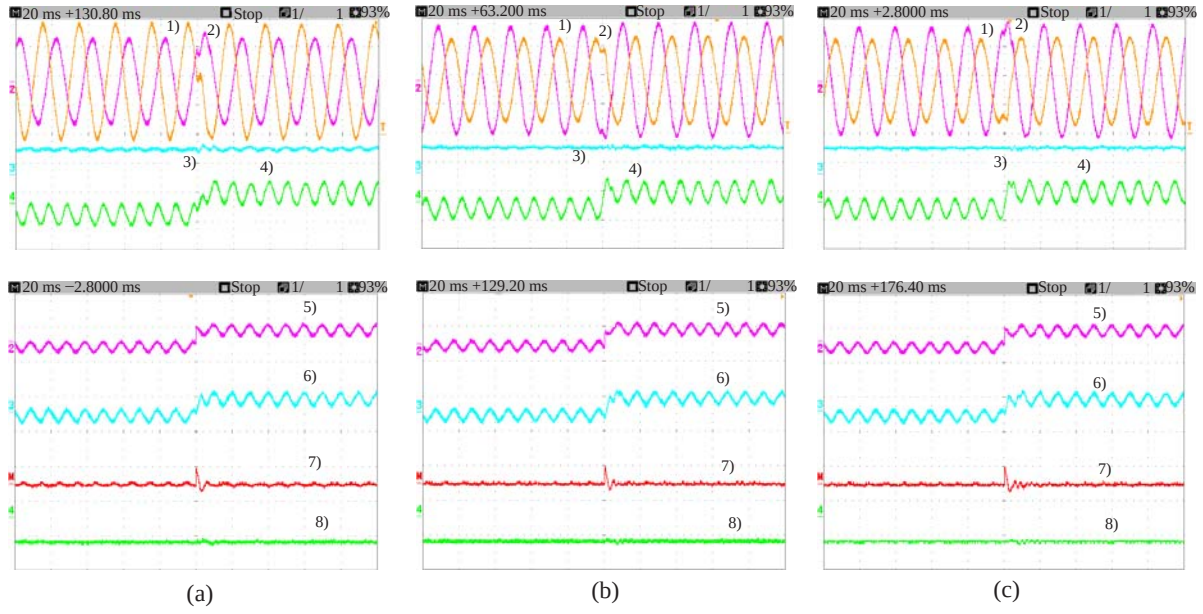

Fig.8 Experimental results with I_{d+}^{+*} =−7.5 A (peak) and I_{q+}^{+*} step changed from −3.0 A (peak) (Q absorbing) to 3.0 A (peak) (Q generating) during 18.0% supply voltage imbalance and 5th and 7th order voltage harmonics being 0.9% and 0.35%, respectively

(a) Single PI; (b) PI plus resonant controller tuned at 100 Hz; (c) PI plus multi-frequency resonant controllers tuned at 100 and 300 Hz. 1) i_a (5 A/div); 2) i_b (5 A/div); 3) P (2 kW/div); 4) Q (2 kvar/div); 5) I_{gq}^{+*} (9 A/div); 6) I_{gq}^{+} (9 A/div); 7) $\Delta I_{gq}^{+} = I_{gq}^{+*} - I_{gq}^{+}$ (9 A/div); 8) I_{gd+}^{+} (9 A/div)

CONCLUSION

A new current control scheme for PWM GC-VSC under imbalanced and distorted supply voltage conditions is proposed. Without involving any sequential current decomposition process, the control scheme is implemented in the positive synchronous reference frame and provides pretty good regulation for positive/negative sequence currents as well as 5th/7th order current harmonics. Experimental results on a prototype GC-VSC demonstrate that the proposed PI+MFR current control scheme presents satisfactory system performance with the active power oscillations and 5th/7th order current harmonics eliminated during supply voltage imbalance and harmonic distortions.

References

Hu, J.B., He, Y.K., 2007. Multi-frequency proportional-resonant (MFPR) current controller for PWM VSC under unbalanced supply conditions. *J. Zhejiang Univ. Sci. A*, **8**(10):1527-1531. [doi:10.1631/jzus.2007.A1527]

Hu, J.B., He, Y.K., 2008. Modelling and control of grid-connected voltage-sourced converters under generalized unbalanced operation conditions. *IEEE Trans. Energy Conv.*, **23**(3):903-913. [doi:10.1109/TEC.2008.921468]

Hu, J.B., He, Y.K., Nian, H., 2007. Enhanced control of DFIG-used back-to-back PWM VSC under unbalanced grid voltage conditions. *J. Zhejiang Univ. Sci. A*, **8**(8):1330-1339. [doi:10.1631/jzus.2007.A1330]

Kazmierkowski, M.P., Krishnan, R., Blaabjerg, F., 2002. Control in Power Electronics: Selected Problems. Academic Press, San Diego, California, USA, p.89-160.

Rioual, P., Pouliquen, H., Louis, J.P., 1996. Regulation of a PWM rectifier in the unbalanced network state using a generalized model. *IEEE Trans. Power Electron.*, **11**(3):495-502. [doi:10.1109/63.491644]

Song, H., Nam, K., 1999. Dual current control scheme for PWM converter under unbalanced input voltage conditions. *IEEE Trans. Ind. Eelectron.*, **46**(5):953-959. [doi:10.1109/41.793344]

Suh, Y., Lipo, T.A., 2006. Control scheme in hybrid synchronous-stationary frame for PWM AC/DC converter under generalized unbalanced operating conditions. *IEEE Trans. Ind. Appl.*, **42**(3):825-835. [doi:10.1109/TIA.2006.873673]

Verdelho, P., Marques, G.D., 1998. DC voltage control and stability analysis of PWM-voltage-type reversible rectifier. *IEEE Trans. Ind. Eelectron.*, **45**(2):263-273. [doi:10.1109/41.681225]

Wu, X.H., Panda, S.K., Xu, J.X., 2008. Analysis of instantaneous power flow for three-phase PWM boost rectifier under unbalanced supply voltage conditions. *IEEE Trans. Power Electron.*, **23**(4):1679-1691. [doi:10.1109/TPEL.2008.925158]

Yin, B., Oruganti, R., Panda, S.K., Bhat, A.K.S., 2008. An output-power-control strategy for a three-phase PWM rectifier under unbalanced supply conditions. *IEEE Trans. Ind. Eelectron.*, **55**(5):2140-2151. [doi:10.1109/TIE.2008.918643]

Yuan, X., Merk, W., Stemmler, H., Allmeling, J., 2002. Stationary-frame generalized integrators for current control of active power filters with zero steady-state error for current harmonics of concern current under unbalanced and distorted operating conditions. *IEEE Trans. Ind. Appl.*, **38**(2):523-532. [doi:10.1109/28.993175]

Zmood, D.N., Holmes, D.G., 2003. Stationary frame current regulation of PWM inverters with zero steay-state error. *IEEE Trans. Power Electron.*, **18**(3):814-822. [doi:10.1109/TPEL.2003.810852]